Supporting Information

Kinetics and Mechanisms of Gas Phase Reactions of Hexenols with Ozone

Xiaoxiao Lin,[1] Qiao Ma,[1,3] Chengqiang Yang, [1,2] Xiaofeng Tang, [1] Weixiong Zhao,[1]

Changjin Hu,[1] Xuejun Gu,[1] Bo Fang,[1] Yanbo Gai,[1,*] Weijun Zhang,[1,2,*]

[1] *Laboratory of Atmospheric Physico-Chemistry, Anhui Institute of Optics and Fine Mechanics, Chinese Academy of Sciences, Hefei, 230031, Anhui, China*

[2] *School of Environmental Science and Optoelectronic Technology, University of Science and Technology of China, Hefei, 230026, Anhui, China*

[3]*University of Science and Technology of China, Hefei 230026, China*

* Corresponding author：

Prof. Weijun Zhang: wjzhang@aiofm.ac.cn

Dr. Yanbo Gai: gaiyanbo@aiofm.ac.cn

SUMMARY:

11 pages, including 9 Figures.

Figure Captions:

Fig. S1 Concentration measurement of (E)-2-hexen-1-ol by GC/FID in absence of O_3 (values used here were from the integrated peak areas, which were proportional to the concentration of the measured hexenol).

Fig. S2 Pseudo-first-order plots for O_3 reactions with different concentrations of (E)-3-hexen-1-ol (in molecule cm^{-3}).

Fig. S3 Pseudo-first-order plots for O_3 reactions with different concentrations of (E)-4-hexen-1-ol (in molecule cm^{-3}).

Fig. S4 Pseudo-first-order plots for O_3 reactions with different concentrations of (Z)-2-hexen-1-ol (in molecule cm^{-3}).

Fig. S5 Pseudo-first-order plots for O_3 reactions with different concentrations of (Z)-3-hexen-1-ol (in molecule cm^{-3}).

Fig. S6 Pseudo-first-order plots for O_3 reactions with different concentrations of (Z)-4-hexen-1-ol (in molecule cm^{-3}).

Fig. S7 Structures of the hexenols optimized at the BH&HLYP/6-31+G(d,p) level of theory.

Fig. S8 Schematic potential energy surface for the reactions of (E)-3-hexen-1-ol and (Z)-3-hexen-1-ol with O_3 at the BH&HLYP/6-31+G(d,p) level of theory (in kcal/mol).

Fig. S9 Schematic potential energy surface for the reactions of (E)-4-hexen-1-ol and (Z)-4-hexen-1-ol with O_3 at the BH&HLYP/6-31+G(d,p) level of theory (in kcal/mol).

Fig. S1

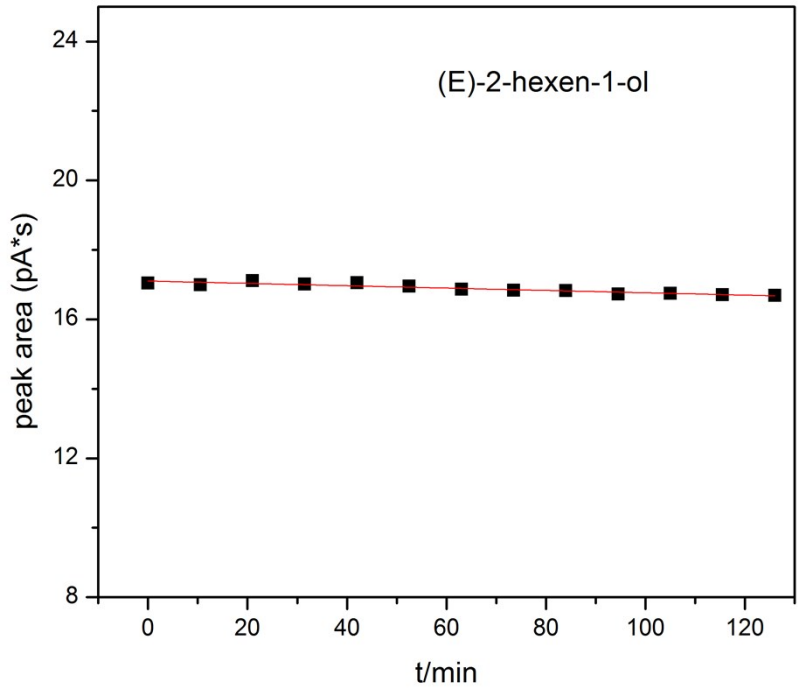

Wall loss experiments were studied by measuring the decrease of the integrated peak areas using a GC/FID (GC7820A, Agilent Technologies). As can be seen from Fig.S1, within the typical time span of the O_3 reaction experiments (less than half an hour) in this work, the decrease of the integrated peak areas measured by GC/FID was below 0.2% of their initial values, which could be neglected. Even after 2 hours, the decrease was still smaller than 3% of their initial values. So, the wall loss of (E)-2-hexen-1-ol in our experiments could be negligible.

Fig. S2

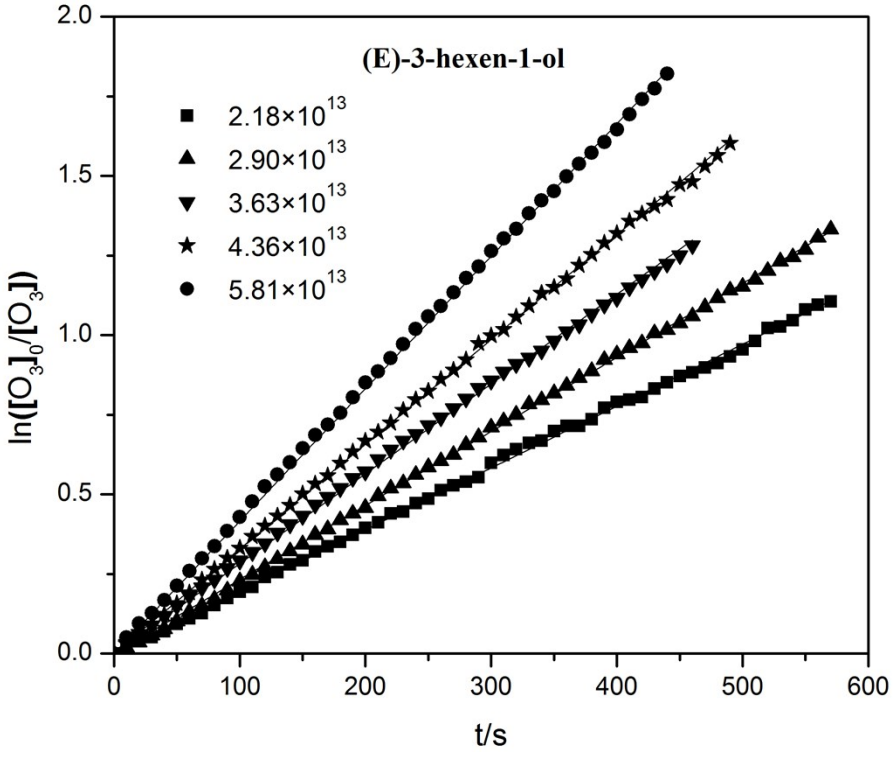
(E)-3-hexen-1-ol
2.18×10^13
2.90×10^13
3.63×10^13
4.36×10^13
5.81×10^13
ln([O3]0/[O3])
t/s
0.0
0.5
1.0
1.5
2.0
0
100
200
300
400
500
600

Fig. S3

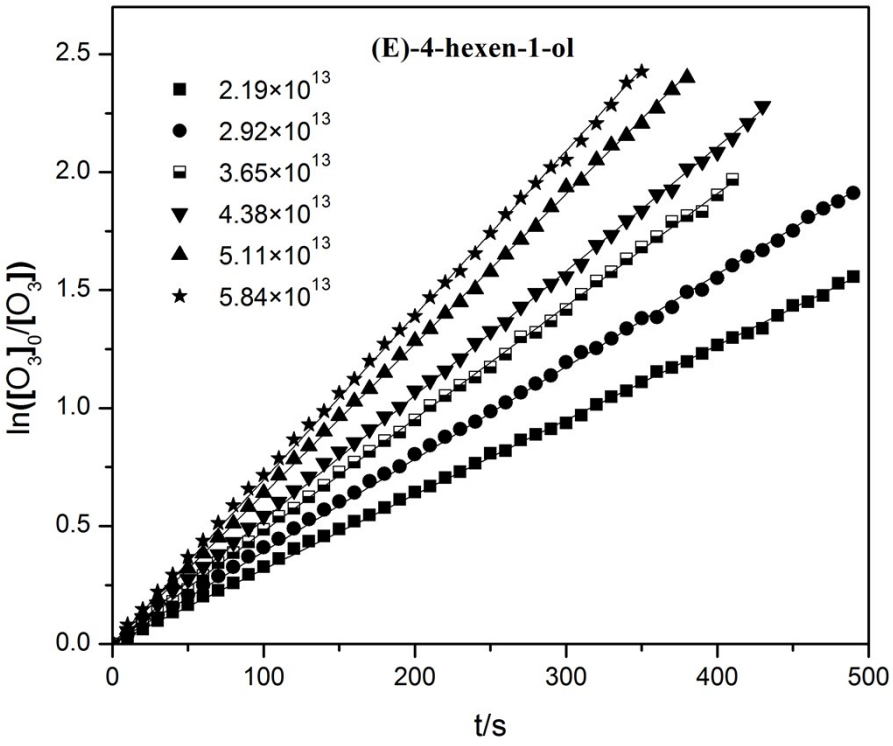
(E)-4-hexen-1-ol
2.19×10^13
2.92×10^13
3.65×10^13
4.38×10^13
5.11×10^13
5.84×10^13
ln([O3]0/[O3])
t/s
0.0
0.5
1.0
1.5
2.0
2.5
0
100
200
300
400
500

Fig. S4

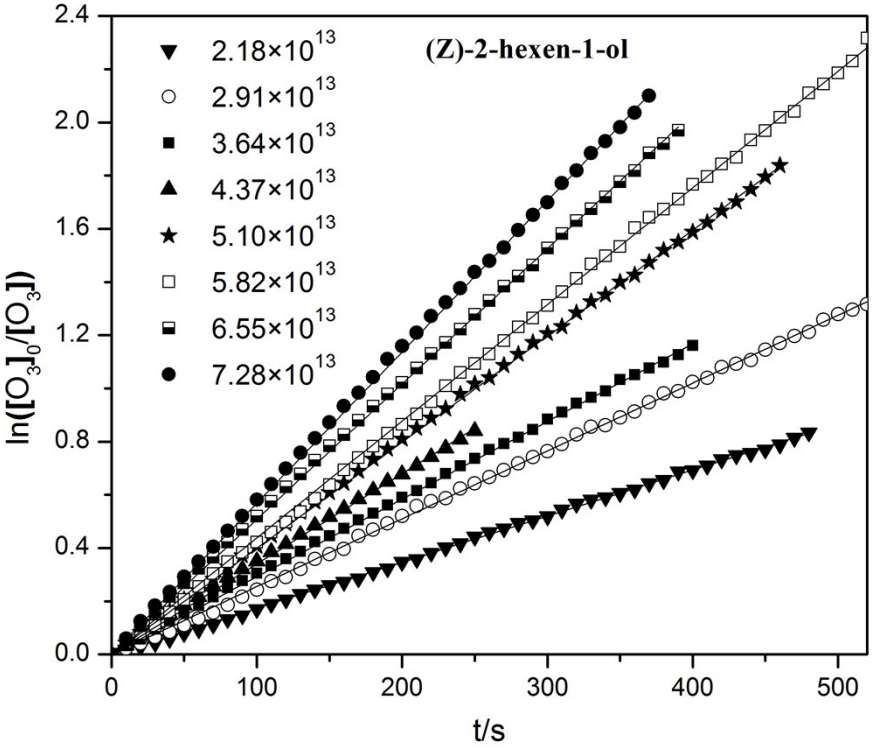
(Z)-2-hexen-1-ol
2.18×10^13
2.91×10^13
3.64×10^13
4.37×10^13
5.10×10^13
5.82×10^13
6.55×10^13
7.28×10^13
ln([O3]0/[O3])
t/s
0.0
0.4
0.8
1.2
1.6
2.0
2.4
0
100
200
300
400
500

Fig. S5

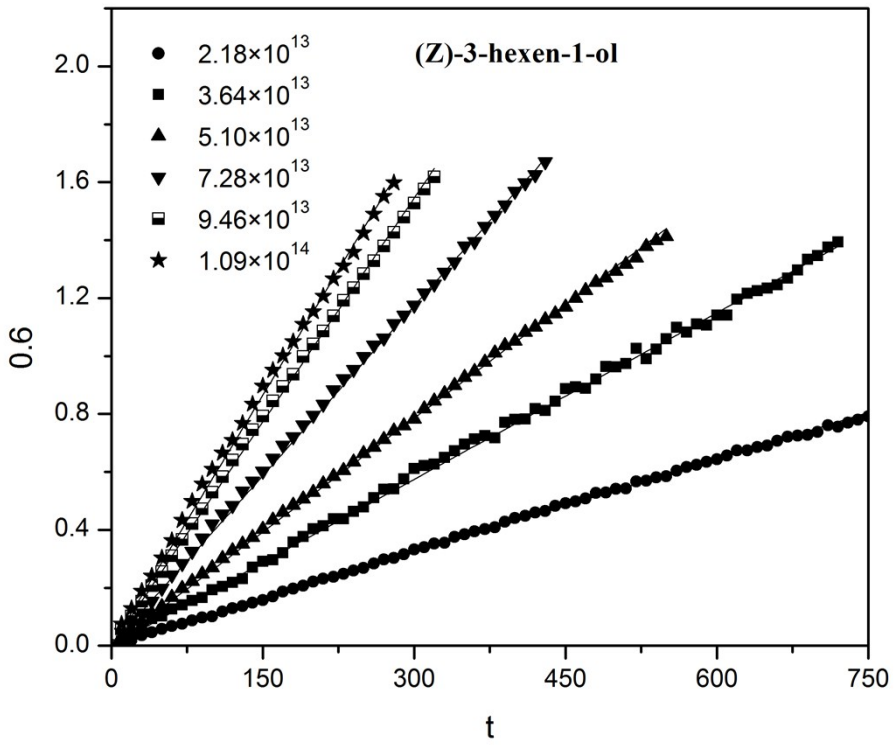
(Z)-3-hexen-1-ol
2.18×10^13
3.64×10^13
5.10×10^13
7.28×10^13
9.46×10^13
1.09×10^14
0.6
0.0
0.4
0.8
1.2
1.6
2.0
0
150
300
450
600
750
t

Fig. S6

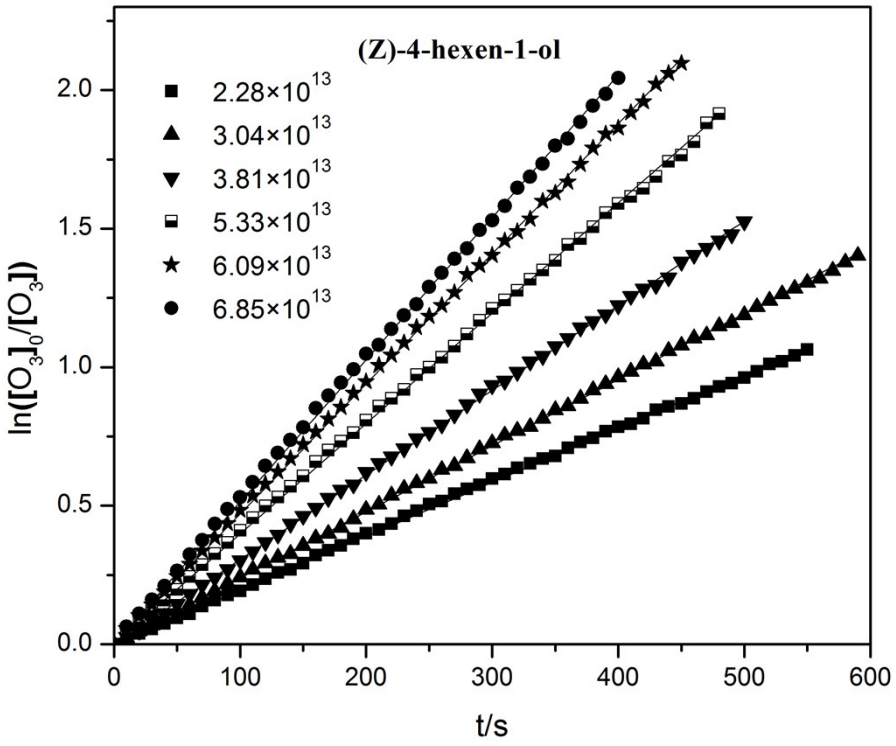
(Z)-4-hexen-1-ol
2.28×10^13
3.04×10^13
3.81×10^13
5.33×10^13
6.09×10^13
6.85×10^13
ln([O3]0/[O3])
t/s
0.0
0.5
1.0
1.5
2.0
0
100
200
300
400
500
600

Fig. S7

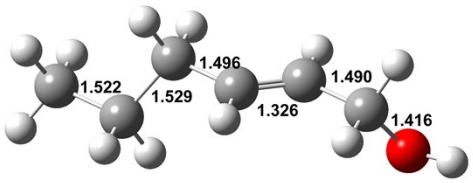

(E)-2-hexen-1-ol

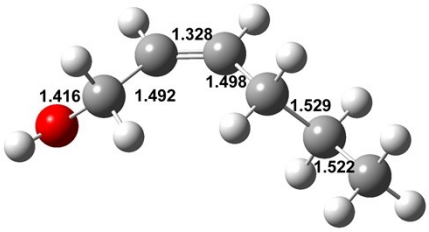

(Z)-2-hexen-1-ol

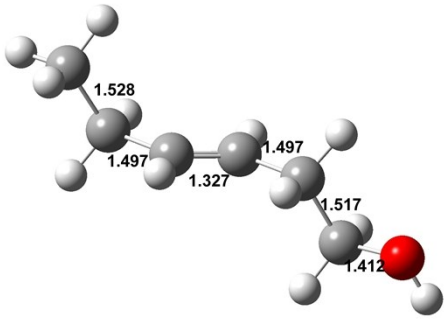

(E)-3-hexen-1-ol

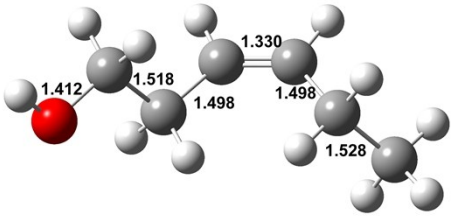

(Z)-3-hexen-1-ol

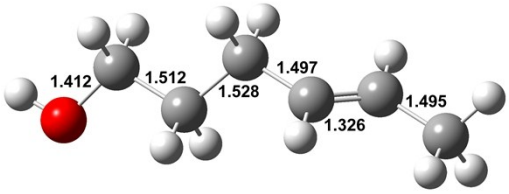

(E)-4-hexen-1-ol

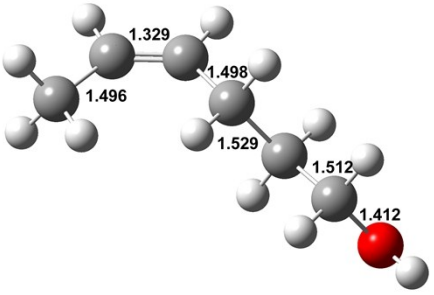

(Z)-4-hexen-1-ol

Fig. S8

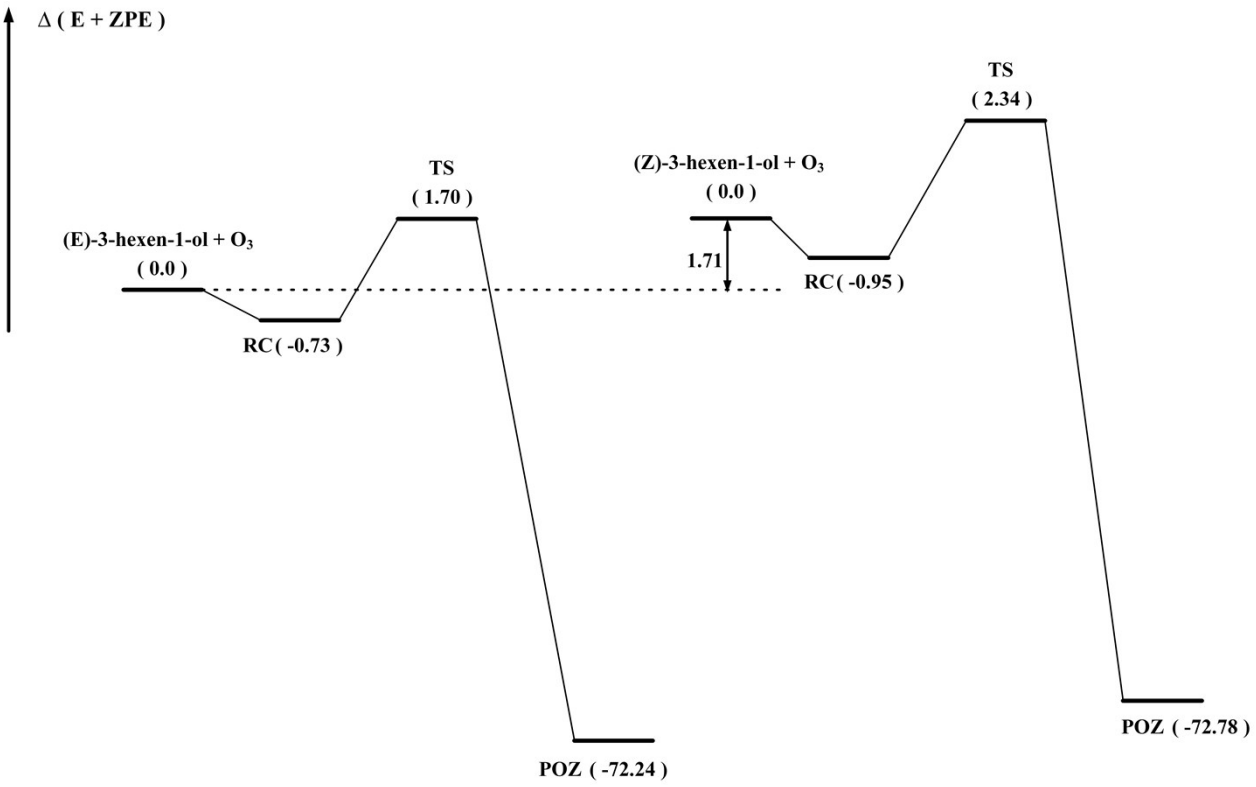
Δ (E + ZPE)
(E)-3-hexen-1-ol + O3
(0.0)
RC (-0.73)
TS
(1.70)
POZ (-72.24)
(Z)-3-hexen-1-ol + O3
(0.0)
1.71
RC (-0.95)
TS
(2.34)
POZ (-72.78)

Fig. S9

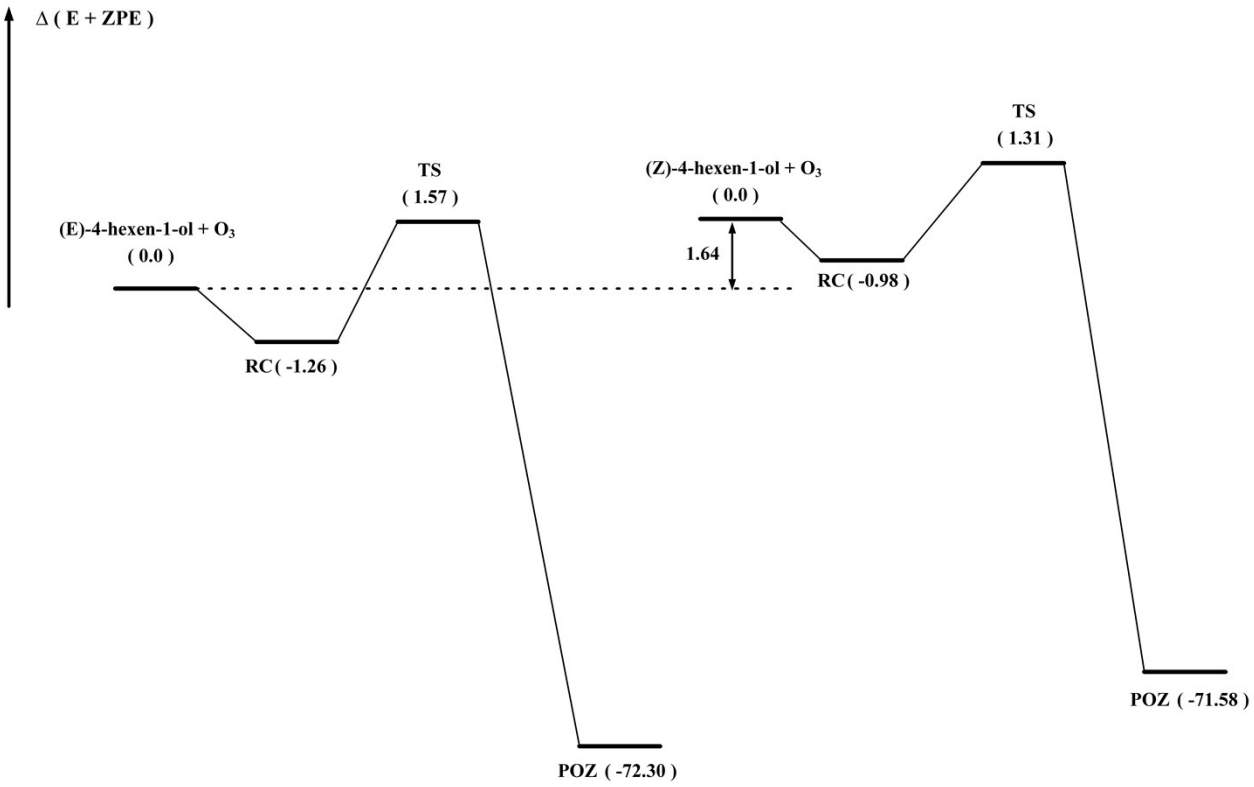
Δ (E + ZPE)
(E)-4-hexen-1-ol + O3
(0.0)
TS
(1.57)
RC (-1.26)
POZ (-72.30)
(Z)-4-hexen-1-ol + O3
(0.0)
1.64
RC (-0.98)
TS
(1.31)
POZ (-71.58)